J Toxicol Pathol 2024; 37: 139–149

Original Article

Protein overexpression by adeno-associated virus-based gene therapy products in cardiomyocytes induces endoplasmic reticulum stress and myocardial degeneration in mice

Kyohei Yasuno[1*], Ryo Watanabe[1], Rumiko Ishida[1], Keiko Okado[2], Hirofumi Kondo[3], Takuma Iguchi[1], Masako Imaoka[1], and Yoshimi Tsuchiya[1]

[1] Medicinal Safety Research Laboratories, Daiichi Sankyo Co., Ltd., 1-16-13 Kita-Kasai, Edogawa-ku, Tokyo 134-8630, Japan
[2] Department of Translational Research, Daiichi Sankyo RD Novare Co., Ltd., 1-16-13 Kita-Kasai, Edogawa-ku, Tokyo 134-8630, Japan
[3] Discovery Research Laboratories IV, Daiichi Sankyo Co., Ltd., 1-2-58 Hiromachi, Shinagawa-ku, Tokyo 140-8710, Japan

Abstract: Gene therapy (GT) products created using adeno-associated virus (AAV) vectors tend to exhibit toxicity via immune reactions, but other mechanisms of toxicity remain incompletely understood. We examined the cardiotoxicity of an overexpressed transgenic protein. Male C57BL/6J mice were treated with a single intravenous dose of product X, an AAV-based GT product, at 2.6×10^{13} vg/kg. Necropsies were performed at 24 h, 7 days, and 14 days after dosing. Pathological examination and gene expression analysis were performed on the heart. Histopathologically, hypertrophy and vacuolar degeneration of cardiomyocytes and fibrosis were observed 14 days after dosing. Immunohistochemistry for endoplasmic reticulum (ER) stress-related proteins revealed increased positive reactions for glucose-regulated protein 78 and C/EBPR homologous protein in cardiomyocytes 7 days after dosing, without histopathological abnormalities. Fourteen days after dosing, some cardiomyocytes showed positivity for PKR-like endoplasmic reticulum kinase and activating transcription factor 4 expression. Ultrastructurally, increases in the ER and cytosol were observed in cardiomyocytes 7 days after dosing, along with an increase in the number of Golgi apparatus compartments 14 days after dosing. The tissue concentration of the transgene product protein increased 7 days after dosing. Gene expression analysis showed upregulation of ER stress-related genes 7 days after dosing, suggesting activation of the PKR-like ER kinase pathway of the unfolded protein reaction (UPR). Thus, the cardiotoxicity induced by product X was considered to involve cell damage caused by the overexpression of the product protein accompanied by UPR. Marked UPR activation may also cause toxicity of AAV-based GT products. (DOI: 10.1293/tox.2024-0011; J Toxicol Pathol 2024; 37: 139–149)

Key words: gene therapy, adeno-associated virus, cardiac degeneration, unfolded protein reaction, cardiotoxicity, mouse

Introduction

Gene therapy (GT) is a technique that modifies a person's genes to treat a disease by introducing a new or modified gene into the body. Viruses are often used as vectors to deliver target genes to patients' cells, and in recent years adeno-associated virus (AAV) vectors have become a widely used option to achieve this because of their advantages in terms of safety, tissue tropism, and highly efficient introduction of genes[1–3]. AAV is a nonpathogenic single-stranded DNA parvovirus that is unable to replicate by itself[1, 3]. In nature, AAV exists as at least 13 different serotypes, each of which is known to have different tropisms in tissues[1–3]. AAV vectors consist of two components: a protein capsid and an internal DNA construct[1]. The DNA in AAV vectors is modified from the wild-type by removing the genes responsible for replication and capsid formation and replacing them with promoters or enhancers that drive the expression of a gene of interest[1, 2]. The efficiency of infection through the tissue tropism of AAV and the efficiency of gene introduction through the promoters or enhancers are important for expressing the transgene protein products (hereafter referred to as "target proteins") in the target cells[1–3].

Findings from clinical and non-clinical studies have shown that AAV-based GT products cause toxicity to many organs and tissues, including the liver, kidney, heart, neurons, and platelets in blood[4–11]. Most of these toxicities are considered to involve immune responses against AAV vectors and/or the target proteins that they produce. For example, liver-associated adverse events, including serious acute liver injury, have been found in clinical studies of onase-

Received: 6 February 2024, Accepted: 20 May 2024
Published online in J-STAGE: 7 June 2024
*Corresponding author: K Yasuno
(e-mail: kyohei.yasuno@daiichisankyo.com)

mnogene abeparvovec, an AAV-based GT product used for treating spinal muscular atrophy[4]. Preclinical studies suggested an excessive immune response to the vector capsid as a possible mechanism underlying these events. However, toxic mechanisms other than the activation of the immune responses remain poorly understood.

In the present study, we characterized cardiotoxicity as being related to the overexpression of a target protein by administering the AAV-based GT product X to mice. We performed a detailed pathological examination and gene expression analysis to show that the overexpression of target proteins can induce toxicity without activating immune responses via an increase in endoplasmic reticulum (ER) stress.

Materials and Methods

Animals

Male C57BL/CJ mice (n=29; The Jackson Laboratory Japan, Inc., Yokohama, Japan) aged three weeks were used in this study. The animals were housed in conventional cages (2–4 per cage) in an animal study room with the temperature controlled at 20–26°C, humidity of 30%–70%, and a 12-h light (150–325 lux)/12-h dark cycle. A certified pellet diet (FR-2; Funabashi Farm Co., Chiba, Japan) and chlorine-added tap water were provided *ad libitum*. All studies were approved by the Ethics Review Committee for Animal Experimentation of Daiichi Sankyo Co., Ltd. and were performed in accordance with the guidelines of the Animal Care and Use Committee of Daiichi Sankyo Co., Ltd. The experiments were also performed in compliance with laws or guidelines relating to animal welfare, including the Standards Relating to the Care and Management of Experimental Animals (Notification No. 6 of the Prime Minister's Office, Japan; March 27, 1980) and the Guidelines for Animal Experimentation (Japanese Association for Laboratory Animal Science; May 22, 1987).

Test compound and study design

The AAV-based GT product X (product X), which was manufactured by Daiichi Sankyo Co., Ltd. (Tokyo, Japan), was used in this study. Phosphate-buffered saline (PBS; FUJIFILM Wako Pure Chemical Corporation, Osaka, Japan) or product X dissolved in PBS was injected intravenously into mice at a dose of 2.6×10^{13} vg/kg. This dose was based on the findings of a preliminary study in which cardiotoxicity was induced at a similar dosage. The animals were euthanized 24 h, and 7 and 14 days after exsanguination under isoflurane anesthesia. Four animals were used in each group, but for the groups analyzed 7 days after dosing, additional animals were included in the control (PBS-treated group, N=3) and product X-treated (N=2) groups for gene expression analysis (see "*Gene expression analysis in heart*").

Histopathology

The hearts, livers, and lungs were collected during necropsy. The heart was sectioned coronally, and the sample of its ventral half, which included the bilateral atria and ventricles, was fixed in 10% neutral-buffered formalin (NBF). The medial right and left lobes of the liver and the whole lung were also fixed in 10% NBF. The dorsal half of the heart and remaining tissues of the liver were immediately frozen in liquid nitrogen and stored at −80°C for use in measuring the vector gDNA and target protein concentrations and for gene expression analysis. Fixed tissues were embedded in paraffin, sectioned, and stained with hematoxylin and eosin staining.

Immunohistochemistry

Immunohistochemistry for glucose-regulated protein 78 (GRP78), PKR-like endoplasmic reticulum kinase (PERK), activating transcription factor 4 (ATF4), C/EBP homologous protein (CHOP), cleaved-caspase 3, CD3, CD45RA, and F4/80 was performed in the hearts and livers in the control and product X-treated groups, in accordance with the previously reported protocol[12, 13] using a Leica Biosystems BOND® RXm instrument (Leica Biosystems, Wetzlar, Germany). Following incubation with Protein Block Serum-Free (Dako, Agilent Technologies, Inc., Santa Clara, CA, USA), dewaxed sections were incubated with antibodies. The detailed staining conditions are summarized in Table 1. After immunoreaction with secondary antibodies, the sections were stained with diaminobenzidine and counterstained with Mayer's hematoxylin.

Electron microscopic examination

Portions of 10% NBF-fixed tissue specimens from the heart of the control group (n=2, 7 days after dosing) and product X-treated group (n=2 each, 7 and 14 days after dosing) were cut into cubes of 1 mm^3, refixed in 2.5% glutaraldehyde, and post-fixed in 1% OsO_4 for 2 h. The specimen was then dehydrated using an ascending concentration gradient of alcohol and embedded in epoxy resin. Ultrathin sections were double-stained with uranyl acetate and lead citrate and examined using an H-7500 transmission electron microscope (Hitachi High-Technologies Corporation, Tokyo, Japan) at 80 kV.

Preparation of tissue lysate

Tissue lysates were prepared for use in measuring vector gDNA and target protein concentrations in tissues and for gene expression analyses. Frozen heart and liver tissues were mixed in 4% SDS, 4 M urea, and 125 mM Tris-HCl solution and homogenized five times for 2 min each with tungsten beads (Biomedical Science Co., Ltd., Tokyo, Japan) and zirconia balls (Nikkato Corporation, Osaka, Japan) using a tabletop bead crusher (Shake Master Neo, BMS-M10N21; Biomedical Science Co., Ltd.) at 1,500 rpm. Samples were centrifuged at 10,000 × g for 10 min at 4°C, and the supernatant was further centrifuged at 12,000 × g for 10 min at 4°C. Then, the supernatant was heated for 10 min at 95°C to inactivate AAV. Samples were subsequently frozen in liquid nitrogen and stored at −80°C until use.

Table 1. Antibodies Used for Iimmunohistochemistry and Brief Protocol

Primary antibody				Secondary antibody		Antigen retrieval
	Clone	Dilution	Source		Source	
GRP78	Polyclonal	1:1000	GeneTex Inc., Irvine, CA, USA	EnVision+ System-HRP-Labeled Polymer Anti-Rabbit	Dako Agilent Technologies, Inc., Santa Clara, CA, USA	No treatment
PERK	Polyclonal	1:85	Abcam plc, Cambridge, UK	EnVision+ System-HRP-Labeled Polymer Anti-Rabbit	Dako Agilent Technologies, Inc., Santa Clara, CA, USA	98°C, 20 min, pH 6.0
ATF4	Polyclonal	1:100	Abcam plc, Cambridge, UK	EnVision+ System-HRP-Labeled Polymer Anti-Rabbit	Dako Agilent Technologies, Inc., Santa Clara, CA, USA	98°C, 20 min, pH 6.0
CHOP (DDIT3)	9C8	1:200	Abcam plc, Cambridge, UK	Mouse on Mouse Polymer IHC kit	Abcam plc, Cambridge, UK	No treatment
Cleaved-caspase 3	Asp175	1:500	Cell Signaling Technology, Inc., Danvers, MA, USA	Mouse on Mouse Polymer IHC kit	Abcam plc, Cambridge, UK	98°C, 20 min, pH 6.0
CD3	SP7	1:100	Abcam plc, Cambridge, UK	Mouse on Mouse Polymer IHC kit	Abcam plc, Cambridge, UK	98°C, 20 min, pH 6.0
CD45RA	RA3-6B2	1:100	Becton, Dickinson and Company, Franklin Lakes, NJ, USA	Mouse on Mouse Polymer IHC kit	Abcam plc, Cambridge, UK	98°C, 20 min, pH 9.0
F4/80	CI:A3-1	1:100	Abcam plc, Cambridge, UK	Goat Anti-Rat IgG H&L HRP Polymer	Abcam plc, Cambridge, UK	No treatment

GRP78: glucose-regulated protein 78; PERK: PKR-like endoplasmic reticulum kinase; CHOP: C/EBP homologous protein; DDIT3: DNA damage-inducible transcript 3; ATF4: activating transcription factor 4. pH 6.0: citrate buffer; pH 9.0: Tris/EDTA buffer.

Measurement of vector gDNA concentration in the heart and liver

After treatment with RNase, DNA was extracted from the tissue lysates of the heart and liver using the magnetic bead method using the MagMAX DNA Multi-Sample Ultra Kit 2.0 (Applied Biosystems, Thermo Fisher Scientific Inc., Waltham, MA, USA) and the KingFisher FLEX system (Thermo Fisher Scientific Inc.). After measuring the total DNA concentration using a Qubit Flex Fluorometer (Thermo Fisher Scientific Inc.), the vector gDNA concentration in the extracted DNA solution was measured using the TaqMan probe method. Absolute quantification of vector gDNA was performed using standard curves created using samples of DNA standards at known concentrations. TaqMan Fast Advanced Master Mix (Thermo Fisher Scientific Inc.) was used as the qPCR master mix, and measurements were performed using the CFX96 Real-Time PCR System (Bio-Rad Laboratories, Inc., Hercules, CA, USA). Data are expressed as the mean ± standard deviation.

Measurement of target protein concentration in the heart and liver

The total protein concentration in the tissues was measured following the protocol of the Micro BCA Protein Assay kit (Thermo Fisher Scientific Inc.), and 200 μg of total protein was collected in tubes from the tissue lysates of each sample prepared in *Preparation of tissue lysate*. After adding 10 μL of 10% 1 M Tris-HCl (pH 8.0), 20% acetonitrile solution, and an appropriate amount of 2-propanol, the samples were vortexed and centrifuged at 15,000 × g for 15 min at 4°C. Next, the supernatant was removed, and the remaining precipitate was dried at room temperature for a few minutes. Trypsin digestion was performed by reacting the samples at 37°C with 50 μL of 10% 1 M Tris-HCl (pH 8.0), 10% acetonitrile solution, and 4 μL of trypsin/Lys-C Mix, Mass Spec. Grade (1 μg/μL; Promega Co., Ltd., Madison, WI, USA). An internal standard peptide of the transgene protein product (synthesized by SCRAM Co., Ltd., Tokyo, Japan, using stable isotope-labeled amino acids) was added to the tryptic digest, followed by extraction with a solid-phase column (InertSep C2; GL Sciences, Inc., Tokyo, Japan), and the target protein-specific tryptic peptide contained in the sample was analyzed using a liquid chromatograph (Nexera; Shimadzu Corporation, Kyoto, Japan) and a mass spectrometer (QTRAP6500+; SCIEX, Framingham, MA, USA). Absolute quantification of the target protein was performed using standard curves created with standard samples containing the target protein at known concentrations. The quantitative value was converted to the amount of target protein per 1 μg of total protein based on the total protein amount subjected to protein quantification. Data are expressed as the mean ± standard deviation.

Gene expression analysis in the heart

Total RNA was extracted from heart tissue lysates using the RNeasy Mini QIAcube Kit (QIAGEN N.V., Venlo, Netherlands). After measuring the concentration using a multichannel spectrometer (Dropsense 16; Trinean NV/SA, Ghent, Belgium), the samples were stored frozen at −80°C until the reverse-transcription reaction. Since a sufficient amount of total RNA could not be extracted from the heart tissue lysate of the product X-treated group 7 days after dosing using the above method, heart samples were collected from additional mice treated with PBS or product X 7 days after dosing. The fresh hearts were mixed with TRIzol reagent (Thermo Fisher Scientific Inc.), and total RNA was extracted in accordance with the manufacturer's protocol. The obtained total RNA sample was subjected to cDNA and cRNA synthesis using GeneChip 3′IVT PLUS Reagent Kit (Affymetrix, Thermo Fisher Scientific Inc.).

Gene expression analysis was performed using the Clariom S Assay, Mouse (Thermo Fisher Scientific Inc.). Differentially expressed genes were selected using the criteria of fold change >2 and adjusted p-value <0.05 in the product X-treated group compared with the control group at each time point and analyzed with Transcriptome Analysis Console software version 4.0 (Thermo Fisher Scientific Inc.). Data were imported into the Ingenuity Pathway Analysis (IPA; Tomy Digital Biology Co., Ltd., Tokyo, Japan) and BaseSpace Correlation Engine (Illumina Co., Ltd., San Diego, CA, USA) to investigate the functional pathways and genes related to the dosing of product X.

Results

Pathological examination

No abnormal clinical signs were observed in any of the animals until necropsy. At necropsy, hydrothorax was observed in two of the four animals in the product X-treated group 14 days after dosing. Histopathologically, no changes were observed in the heart or liver 24 h or 7 days after dosing (Fig. 1A) or in the lungs at any necropsy time point. Fourteen days after dosing, apparent hypertrophy and vacuolar degeneration of cardiomyocytes with increased interstitial cells and connective tissue were observed in the heart (Fig. 1B). The interstitial cells were negative for lymphocyte and macrophage markers, namely CD3, CD45RA, and F4/80 (data not shown), implying that they were not inflammatory cells but rather proliferating fibroblasts contributing to interstitial fibrosis. Hypertrophic cardiomyocytes showed increased cell size and enlarged nuclei with prominent nucleoli, but necrosis was not observed. Some of these cardiomyocytes showed vacuolar degeneration with small to large cytoplasmic vacuoles and a halo around the nucleus. In the liver, centrilobular vacuolation and hepatocyte necrosis were observed in the product X-treated group 14 days after dosing (Fig. 2). The vacuoles were large, numbering from one to several per cell, and located adjacent to the nucleus. Some nuclei were displaced by vacuoles and exhibited a crescent shape. The vacuoles contained clear or eosinophilic flocculent materials. There was no correlation between hepatocyte vacuolation and necrotic sites.

Immunohistochemically, some cardiomyocytes were positive for GRP78 and CHOP in the product X-treated group 7 days after dosing, whereas they exhibited no changes upon hematoxylin and eosin staining (Fig. 1C and 1E). Fourteen days after dosing, immunohistochemical analyses with both antibodies revealed an increased number of positively stained cardiomyocytes (Fig. 1D and 1F), and a few cardiomyocytes were positive for PERK and ATF4 (Fig. 1G and 1H). Results for cleaved-caspase 3 were negative at all necropsy time points. In the liver, hepatocytes were negative for GRP78, PERK, CHOP, and cleaved-caspase 3 (ATF4 was not examined).

In the cardiomyocytes of the control mice, the cytoplasm was rich in mitochondria and muscle fibers, and the ER was rarely observed under electron microscopy (Fig. 3A and 3B). Seven days after dosing with product X, there were increases in the ER, especially in the smooth ER and cytosol of cardiomyocytes (Fig. 3C and 3D). Fourteen days after dosing, these changes became more prominent (Fig. 3E and 3F). The findings also revealed an increase in the number of compartments and the overall hypertrophy of the Golgi apparatus (Fig. 3F and 3G).

Vector gDNA and target protein concentrations in the heart and liver

The vector gDNA and target protein concentrations in the heart and liver are shown in Table 2. In the product X-treated group, vector gDNA concentration in the heart decreased over time, showing values of 618 ± 233, 89 ± 40, and 55 ± 10 vg/mg at 24 h, 7 days, and 14 days after dosing, respectively. Conversely, the target protein concentration in the heart increased over time. The obtained results were below the lower limit of quantification (<5 pg/μg of total protein), 152 ± 25.2, and 1,138 ± 402 pg/μg of total protein at 24 h, 7 days, and 14 days after dosing, respectively. The changes in the liver differed from those in the heart. Vector gDNA showed a high concentration 24 h after dosing, which decreased 7 days after dosing. However, 14 days after dosing, the level increased again to match that at 24 h after dosing. The target protein concentration increased over time until 14 days after dosing, but the rate of increase was minimal compared with that in the heart.

Gene expression analysis in the heart

Transcriptomic analysis identified 1,259, 706, and 4,102 differentially expressed genes at 24 h, 7 days, and 14 days after dosing, respectively (Table 3). Specifically, 625, 426, and 2,025 genes were upregulated in the product X-treated group, and 634, 280, and 2,077 genes were downregulated at these time points, respectively.

In the upstream analysis of IPA, we identified the top five activated upstream regulators (Z-score >2) 14 days after dosing in each of the four categories classified by IPA: "transcription regulator", "cytokine", "growth factor", and "others" (Table 4). For these identified upstream regulators, Z-scores were compared at 24 h, 7 days, and 14 days after administration. Twenty-four hours after dosing, there was activation of upstream regulators related to cytokines, namely, interferon-gamma (*Infg*) and tumor necrosis factor (*Tnf*), and a cytosolic sensor of viral DNA, namely stimulator of interferon response cGAMP interactor 1 (*Sting1*)[14]. Seven days after dosing, the results revealed the activation of upstream regulators related to ER stress, namely X-box binding protein 1 (*Xbp1*); related to cardiac remodeling, namely transforming growth factor beta 1 (*Tgfb1*)[15], KLF transcription factor 6 (*Klf6*)[15], and angiotensinogen (*Ang*)[16]; and related to intracellular vesicular trafficking, namely trafficking protein particle complex subunit 1 (*Tappc1*)[17]. Fourteen days after dosing, the activation of *Xbp1*, *Infg*, *Tnf*, *Tgfb1*, *Klf6*, *Ang*, *Sting1*, and *Trappc1* seen at 7 days after dosing was maintained, and additional activation of upstream regulators related to cytokines, such as interleukin 1

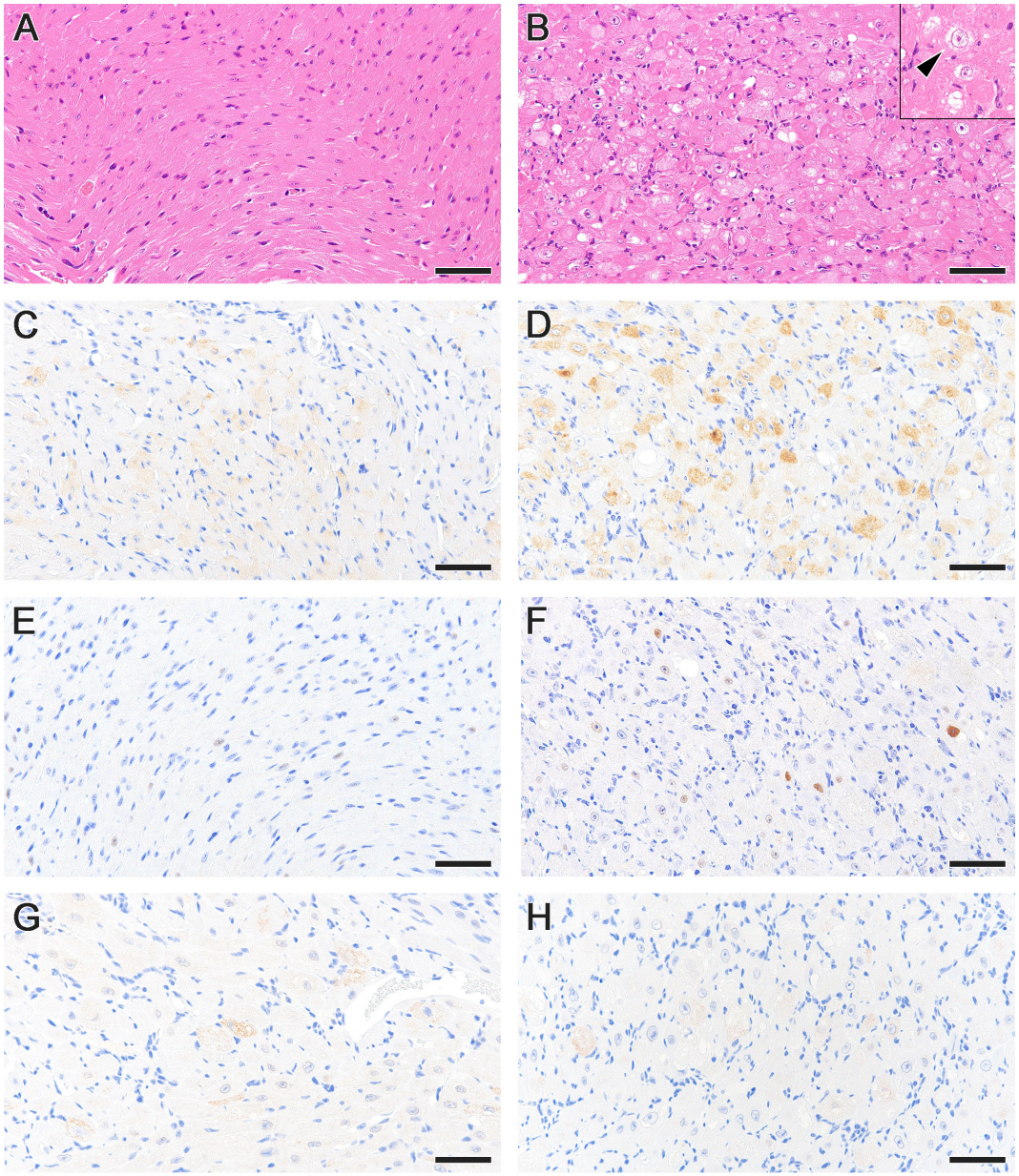

Fig. 1. Histopathology (A and B) and immunohistochemistry (C–H) of the heart of mice treated with a single intravenous dose of 2.6×10^{13} vg/kg of AAV-based gene therapy (GT) product X (A, C, and E, 7 days after dosing; B, D, and F–H, 14 days after dosing). No changes are observed 7 days after dosing (A), whereas apparent hypertrophy and vacuolar degeneration of cardiomyocytes and slight proliferation of fibroblasts with interstitial fibrosis are observed at 14 days after dosing (B). Hypertrophic cardiomyocytes show enlarged nuclei with prominent nucleoli. A halo is observed around the nucleus in some cardiomyocytes (B, inset, arrowhead). Glucose-regulated protein 78 (GRP78)- and C/EBP homologous protein (CHOP)-positive cardiomyocytes are observed 7 (C, GRP78, cytoplasm; E, CHOP, nucleus) and 14 days (D, GRP78; F, CHOP) after dosing. A few PKR-like endoplasmic reticulum kinase (PERK, G, cytoplasm)- or activating transcription factor 4 (ATF4, H, cytoplasm)-positive cells are observed 14 days after dosing. A and B, hematoxylin and eosin (HE) staining; C to H, immunohistochemistry. Bar=100 (A–D) or 50 μm (E–H).

beta (*Il1b*), and related to cardiac remodeling, such as integrin subunit alpha 11 (*Itga11*)[18], was observed.

In the downstream analysis, we identified the top five activated downstream functions (Z-score >2) as phenotypes predicted to be related to myocardial lesions 14 days after dosing (Table 4). For the identified downstream pathways, the Z-scores were compared at 24 h, 7 days, and 14 days after administration. Twenty-four hours after dosing, downstream functions, namely "immune response of cells" and "activation of antigen-presenting cells (APCs)", were activated, whereas none of these functions was activated 7 days after dosing. Fourteen days after dosing, there was the activation of the downstream functions of "proliferation of muscle cells" and "fibrogenesis" related to cardiac remod-

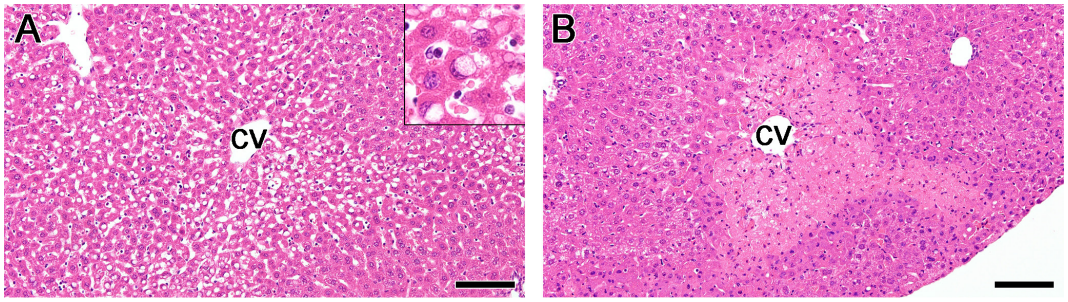

Fig. 2. Histopathology of the liver of mice treated with a single intravenous dose of 2.6×10^{13} vg/kg of AAV-based GT product X. Centrilobular vacuolation (A) and necrosis (B) of hepatocytes are observed 14 days after dosing. Intracytoplasmic vacuoles are irregular in size, and some contain eosinophilic flocculent materials (A, inset). CV, central vein. HE staining. Bar=100 µm.

Table 2. Vector gDNA and Transgene Protein Product (Target Protein) Concentrations in the Heart and Liver in Mice Treated with AAV-based Gene Therapy Product X

		Time after dosing		
		24 h	7 days	14 days
Vector gDNA	(vg/g gDNA)			
Heart		618 ± 234	89 ± 41	55 ± 10
Liver		2,330 ± 510	893 ± 269	2,696 ± 1,386
Target protein	(pg/g total protein)			
Heart		< LLOQ	152 ± 25.2	1,138 ± 402
Liver		5.73 ± 0.382	22.3 ± 3.8	30.5 ± 20.7

LLOQ: lower limit of quantification (5 pg/µg total protein).

Table 3. Number of Differentially Expressed Genes in the Heart in Mice Treated with AAV-based Gene Therapy Product X

	Time after dosing		
	24 h	7 days	14 days
Upregulated	625	426	2,025
Downregulated	634	280	2,077

The number of differentially expressed genes that shows false discovery rate (FDR) p-value <0.05 and absolute log2 fold changes >1 in the product X-treated group compared with the concurrent control group. Gene expression profile of the heart obtained from the animals was analyzed with Clariom S Assay, Mouse (Thermo Fisher Scientific Inc., Waltham, MA, USA) and Transcriptome Analysis Console (TAC) software version 4.0 from Affymetrix, Thermo Fisher Scientific Inc.

eling and also "immune response of cells", "production of reactive oxygen species (ROS)", and "activation of APCs" related to inflammation. No activation of genes or functions related to apoptosis was detected by either upstream or downstream analysis.

In the pathway analysis using the BaseScope Correlation Engine, we identified genes related to the unfolded protein response (UPR) in the ER 14 days after dosing and compared their fold change as calculated from the log signal ratio with the concurrent control group at 24 h, 7 days, and 14 days after dosing (Table 5). The results revealed that UPR genes were upregulated 7 days after dosing, which coincided with the time point at which the expression of CHOP, a transcript of *Ddit3*, was observed using immunohistochemistry. In addition, *Creb3* and *Arf4*, which are genes related to Golgi apparatus stress[19], were upregulated by 4.5- and 3.7-fold, respectively, 14 days after dosing.

Discussion

In this study, a single intravenous injection of the AAV-based GT product X induced the degeneration of cardiomyocytes and slight interstitial fibrosis in the hearts of mice 14 days after dosing. Immunohistochemistry and electron microscopy revealed the expression of ER stress-related proteins and morphological changes in the ER in cardiomyocytes 7 days after dosing, which were considered to reflect the upregulation of UPR genes in gene expression analysis.

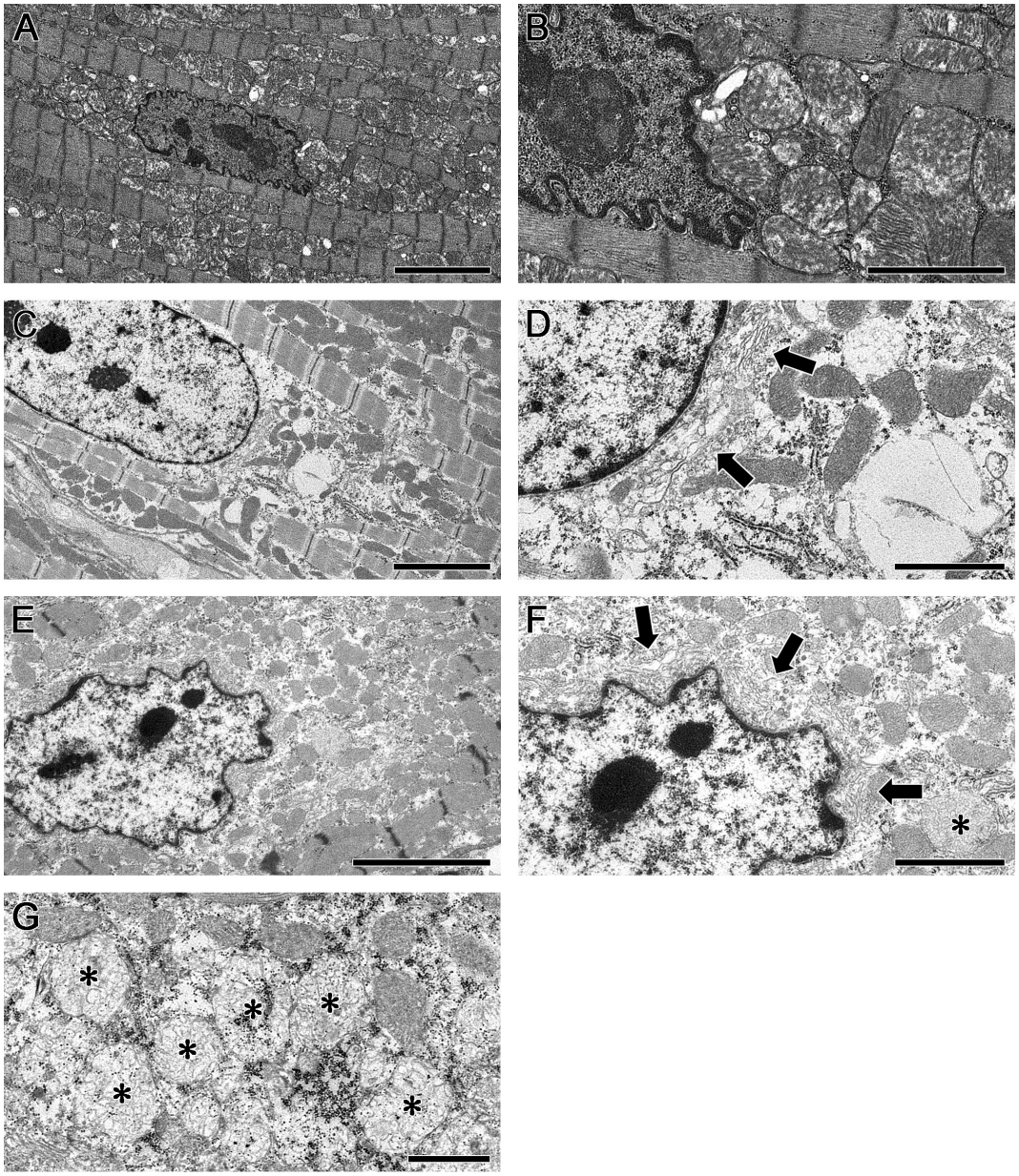

Fig. 3. Electron microscopy of the heart of mice treated with a single intravenous dose of 0 (control, A and B, 7 days after dosing) or 2.6 × 10^{13} vg/kg (C–G) of AAV-based GT product X (C–D, 7 days after dosing; E–G, 14 days after dosing). In the control mice, the cytoplasm is rich in mitochondria and muscle fibers, and the ER is rarely seen (A and B). In AAV-based GT product X-treated mice, an increase in the number of compartments of endoplasmic reticulum (ER), especially smooth ER (D, arrows), and mild expansion of the cytosol are observed 7 days after dosing (C and D). Further increases in the number of compartments of ER (F, arrows show the smooth ER) and the area of the cytosol are observed 14 days after dosing (E and F). An increase in the number of compartments and overall hypertrophy of the Golgi apparatus are also observed (F and G, asterisk). Bar=5 (A, C, and E), 2 (B, D, and F), or 1 μm (G).

Based on these findings, the cardiotoxicity in the present study was considered to be due to the activation of the UPR in cardiomyocytes.

The activation of immune responses has been considered the main cause of toxicity provoked by AAV-based GT products in clinical and non-clinical studies[20, 21]. AAV causes the activation of innate immunity in the early stage of infection and the subsequent induction of adaptive immunity. The activation of innate immunity is considered to involve the stimulation of immune cells and target cells by the AAV capsid or transgene DNA via Toll-like receptors. Upon such activation, each cell releases various cytokines such as type I IFN, TNF-α, IL-1, IL-6, and IL-8[21–24]. In this study, the activation of *Tnf* and *Il1b* was observed 24 h after dosing by upstream analysis, but immune cell infiltration was not observed at this time point. Antigen presentation via major histocompatibility complex classes I and II induces antibody-mediated immunity, including the production

Table 4. Ingenuity Pathway Analysis (IPA) for Predicting Upstream Regulators and Downstream Functions in Mice Treated with AAV-based Gene Therapy Product X

Gene	Gene description	Time after dosing		
		24 h	7 days	14 days
Upstream regulators				
Transcription regulators				
Xbp1	X-box binding protein 1	ND	6.4	7.2
Klf6	KLF transcription factor 6	ND	2.2	6.0
Nfe2L2	NFE2-like bZIP transcription factor 2	ND	2.3	5.9
Tp53	tumor protein p53	3.1	2.3	5.8
Bhlhe40	basic helix-loop-helix family member e40	2.7	ND	5.6
Cytokines				
Ifng	interferon gamma	5.0	ND	6.5
Tnf	tumor necrosis factor	3.4	3.6	6.4
Il1b	interleukin 1 beta	ND	2.0	5.3
Prl	prolactin	3.8	ND	5.2
Cntf	ciliary neurotrophic factor	2.0	ND	4.7
Growth factors				
Tgfb1	transforming growth factor beta 1	−3.1	3.9	8.1
Agt	angiotensinogen	ND	3.3	7.7
Angpt2	angiopoietin 2	ND	2.8	4.6
Gdf2	growth differentiation factor 2	ND	ND	3.5
Nrg1	neuregulin 1	ND	3.0	3.3
Others				
Them6	thioesterase superfamily member 6	ND	4.2	4.5
Hax1	HCLS1-associated protein X-1	ND	ND	4.3
Sting1	stimulator of interferon response cGAMP interactor 1	4.7	ND	4.3
Itga11	integrin subunit alpha 11	ND	ND	3.6
Trappc1	trafficking protein particle complex subunit 1	ND	4.2	3.5
Downstream functions				
Proliferation of muscle cells		ND	ND	3.8
Immune response of cells		2.5	ND	3.8
Production of reactive oxygen species		ND	ND	2.7
Activation of antigen-presenting cells		2.0	ND	2.4
Fibrogenesis		ND	ND	2.2

IPA was performed to understand gene functions and regulatory pathways based on differentially expressed genes. The value indicates the activation Z-score, which was calculated from the concordance of the known effects of upstream regulators or downstream functions based on the literature and compiled in the Ingenuity Knowledge Base. Predicted status of upstream regulators was determined by the Z-score (>2, activation; <–2, inhibition) based on the direction of expression change of unigenes in the dataset. ND: not determined.

of anti-AAV antibodies against AAV vectors and antibodies against target proteins. Cell-mediated immunity in the form of the activation of killer T cells is also important for adaptive immunity; these cells are thought to be responsible for the liver injury reported in clinical trials of AAV-based GT products[21, 23, 24]. In the present study, downstream analysis revealed an increased cellular immune response and APC activation at 24 h and 14 days after dosing, but immune cell infiltration was not apparent at the same time points. It was thus considered that the activation of immune responses was less likely to be responsible for the cardiotoxicity observed in this study. The activation of immune responses observed by downstream analysis 14 days after dosing was considered to be a secondary response to the cardiomyocyte degeneration and proliferation of fibroblasts. In future work, the details of the immune responses should be investigated using immune cells, such as peripheral blood mononuclear cells.

The administration of product X induced an increase in ER stress in the heart. ER stress is reported to be involved in the onset and progression of heart failure[25]. Studies using cardiac samples from patients with heart failure have shown that ER stress factors such as GRP78, XBP1, and CHOP increase during heart failure, and increases in GPR78 and CHOP have also been observed in mouse heart failure models[26]. In the present study, increased expression of ER stress proteins and ultrastructural changes in the ER were observed 7 days after dosing, followed by degeneration of cardiomyocytes and slight interstitial fibrosis. Fourteen days after dosing, upstream analysis revealed the activation of cardiac fibrosis-related genes, such as *Tgfb1*, *Klf6*, *Ang*, and *Itga11*[14–16], and downstream analysis revealed the activation of cardiac remodeling, including cardiomyocyte regeneration, interstitial fibrosis, and the activation of ROS production[27]. This sequence of events indicated that ER stress is one of the most important factors in the progression of cardiomyocyte degeneration induced by product X.

The induction of ER stress by GT products using an

Table 5. Differentially Expressed Genes Involved in Endoplasmic Reticulum Unfolded Protein Response in Mice Treated with AAV-based Gene Therapy Product X

Gene	Gene description	Time after dosing		
		24 h	7 days	14 days
Endoplasmic reticulum unfolded protein response				
Hyou1	hypoxia up-regulated 1	NC	25.1	53.8
Dnajc3	DnaJ (Hsp40) homolog, subfamily C, member 3	NC	27.8	38.1
Derl3	Der1-like domain family, member 3	NC	799.3	24.6
Hspa5	heat shock protein 5	NC	5.2	18.9
Ddit3	DNA damage-inducible transcript 3	NC	50.5	18.8
Herpud1	homocysteine-inducible, endoplasmic reticulum stress-inducible, ubiquitin-like domain member 1	NC	6.1	12.6
Atf4	activating transcription factor 4	NC	8.5	12.5
Wfs1	Wolfram syndrome 1 homolog (human)	NC	2.7	10.5
Serp1	stress-associated endoplasmic reticulum protein 1	NC	3.6	8.4
Selenos	histocompatibility 47	NC	NC	6.7
Derl1	Der1-like domain family, member 1	NC	2.3	5.5
Creb3	cAMP-responsive element binding protein 3	NC	NC	4.5
Ero1l	ERO1-like (*S. cerevisiae*)	NC	6.6	3.6
Cdk5rap3	CDK5 regulatory subunit-associated protein 3	NC	NC	3.1
Derl2	Der1-like domain family, member 2	NC	2.3	2.7
Eif2ak2	eukaryotic translation initiation factor 2-alpha kinase 2	2.5	NC	2.6
Creb3l1	cAMP-responsive element binding protein 3-like 1	NC	NC	2.5
Ptpn1	protein tyrosine phosphatase, non-receptor type 1	NC	NC	2.5
Xbp1	X-box binding protein 1	NC	NC	2.2

Differentially expressed genes between control and AAV-based transgene product X-treated mice (t-test, $p<0.05$) that are involved in endoplasmic reticulum unfolded protein response were curated from BaseSpace Correlation Engine. The values indicate the fold change that was calculated from the log signal ratio relative to the concurrent control group. NC: not calculated.

AAV vector has been reported[28]. In that study, an AAV vector expressing recombinant human factor VIII SQ (hFVIII-SQ) with a strong liver-specific promoter was used[28]. ER stress was induced by the increased expression of chaperone proteins such as GRP78, HYOU1, and PDIA1, resulting in the accumulation of hFVIII-SQ in hepatocytes. UPR protein analysis showed increases in ATF6, PDIA4, MANF, and DNAJC3, suggesting the activation of the ATF6 pathway, which is one of the UPR pathways. In the present study, product X induced increased expression of PERK, ATF4, and CHOP, as revealed using immunohistochemistry, and the upregulation of *Ddit3* and *Atf4* in gene expression analysis. These results suggested that the PERK pathway, which is also one of the UPR pathways, was activated by the administration of product X. While no activation of the PERK pathway was reported in the abovementioned study[28], induction of the activation of the UPR pathway by the AAV-GT product was observed, which was reaffirmed in the present study. The discrepancies in the obtained findings may be due to differences in target cells.

Activation of CHOP is known to induce caspase 3-mediated apoptosis[29], but neither immunohistochemistry nor gene expression analysis showed activation of the caspase 3 pathway in the present study. In contrast, hydrothorax, which indicates decreased cardiac function, was observed 14 days after dosing. Changes in the liver also suggested cardiac dysfunction. Rapid dysfunction of the heart was considered to evoke the hepatocellular vacuolation observed 14 days after dosing in the present study, possibly via a decrease in the oxygen supply to the liver, as previously reported[30]. Overall, it was suggested that activation of the UPR in cardiomyocytes induced cardiac dysfunction in the absence of apoptosis. It was speculated that the slight interstitial fibrosis observed 14 days after dosing was a type of cardiac fibrosis known as "reactive fibrosis", characterized by the absence of cardiomyocyte loss[15]. Reactive fibrosis is considered to be an adaptation to cardiac injury to retain the heart's pressure-generating ability. However, the data obtained in this study did not shed light on the mechanism of hepatocellular necrosis. Changes in the vector gDNA and target protein concentrations in the liver were unlikely to be related to hepatotoxicity.

The nature of the target protein is important when considering the induction of ER stress by the GT products. In the abovementioned report by Fong *et al.*[28], the target protein, hFVIII-SQ, was a secreted protein that was considered to be transported outside the cell by exocytosis. In contrast, the target protein in the present study has been reported to localize in the Golgi apparatus in normal muscle cells with no exocytosis. It was speculated that the activation of *Trappc1*, a gene related to intracellular ER-to-Golgi transport[17], 7 days after dosing reflected excess target protein transport inside the cell. Owing to the lack of an exocytosis pathway, it was considered that the target protein would accumulate in the ER and Golgi apparatus. The increase in the number of compartments and overall enlargement of the ER and Golgi apparatus in cardiomyocytes observed in the present study were attributed to the upregulation of target protein synthesis and accumulation of unfolded proteins. However, the reason for the increase in smooth ER was unclear based on the available data.

In the present study, upregulation of *Creb3* and *Arf4*

genes involved in the CREB3 pathway was observed, suggesting activation of the Golgi stress response. The Golgi apparatus has a unique stress response system that is activated in response to cellular demands[19]. When an excess amount of protein is synthesized in the ER and transported to the Golgi apparatus, post-translational modification (PTM) stalls because of a lack of PTM enzymes, followed by the cessation of extracellular transport because of a lack of vesicular transport factors. To address this lack of Golgi apparatus functions, cells accelerate the transcription of genes encoding PTM enzymes and vesicular transport factors by activating the Golgi stress response system. Three pathways for the Golgi stress response have been reported: the CREB3[31], TFE3[32], and HSP47[33] pathways. In the present study, we were unable to confirm the intracellular localization of the target protein immunohistochemically because no appropriate antibodies were available. However, ultrastructural findings in cardiomyocytes at 14 days after dosing, including an increase in the number of compartments, overall enlargement of the ER and Golgi apparatus, and expansion of the cytosol with the migration of myofibers to the periphery of the cell suggested the accumulation of the target protein in the cytosol. The normal structure of cardiomyocytes was almost completely lost, indicating that the accumulation of the target protein may have inhibited the contraction of cardiomyocytes, which is necessary to maintain cardiac functions.

In summary, we showed that GT products created using AAV vectors may cause cell dysfunction by inducing marked UPR activation due to excessive production of the target protein in cardiomyocytes. Target cells of GT products are important factors in assessing the risk associated with the administration of such products. If the target cells have low regenerative potential and are components of a vital organ, such as cardiomyocytes or neurons, inhibition of their functions may cause life-threatening events, even if UPR activation is limited. In fact, a study on non-human primates has described that overexpression of a target protein in neurons induced neuronal necrosis[34]. Accurate estimation of the level of expression of the target protein in the target tissue is thus clearly important before clinical trials can be performed. As GT products can induce irreversible and severe toxicity after a single dose, it is essential to perform an appropriate human risk assessment by considering factors such as the set dose or species differences in the efficiency of gene induction upon AAV infection in target cells in non-clinical studies.

Disclosure of Potential Conflicts of Interest: Kyohei Yasuno, Ryo Watanabe, Rumiko Ishida, Hirofumi Kondo, Masako Imaoka, and Yoshimi Tsuchiya are employees of Daiichi Sankyo Co., Ltd. Keiko Okado is an employee of Daiichi Sankyo RD Novare Co., Ltd.

Acknowledgments: The authors would like to thank Ms. Noriyo Niino (Daiichi Sankyo Co., Ltd.) for performing the gene expression analysis and Dr. Takahiro Suga and Dr. Masashi Hanada (Daiichi Sankyo Co., Ltd.) for measuring the AAV vector gDNA and target protein concentrations.

References

1. Assaf BT, and Whiteley LO. Considerations for preclinical safety assessment of adeno-associated virus gene therapy products. Toxicol Pathol. **46**: 1020–1027. 2018. [Medline] [CrossRef]
2. Hastie E, and Samulski RJ. Adeno-associated virus at 50: a golden anniversary of discovery, research, and gene therapy success--a personal perspective. Hum Gene Ther. **26**: 257–265. 2015. [Medline] [CrossRef]
3. Naso MF, Tomkowicz B, Perry WL 3rd, and Strohl WR. Adeno-associated virus (AAV) as a vector for gene therapy. BioDrugs. **31**: 317–334. 2017. [Medline] [CrossRef]
4. High-dose AAV gene therapy deaths. Nat Biotechnol. **38**: 910. 2020. [Medline] [CrossRef]
5. Chand D, Mohr F, McMillan H, Tukov FF, Montgomery K, Kleyn A, Sun R, Tauscher-Wisniewski S, Kaufmann P, and Kullak-Ublick G. Hepatotoxicity following administration of onasemnogene abeparvovec (AVXS-101) for the treatment of spinal muscular atrophy. J Hepatol. **74**: 560–566. 2021. [Medline] [CrossRef]
6. Chand DH, Zaidman C, Arya K, Millner R, Farrar MA, Mackie FE, Goedeker NL, Dharnidharka VR, Dandamudi R, and Reyna SP. Thrombotic microangiopathy following onasemnogene abeparvovec for spinal muscular atrophy: a case series. J Pediatr. **231**: 265–268. 2021. [Medline] [CrossRef]
7. Duan D. Systemic AAV micro-dystrophin gene therapy for Duchenne muscular dystrophy. Mol Ther. **26**: 2337–2356. 2018. [Medline] [CrossRef]
8. Hinderer C, Katz N, Buza EL, Dyer C, Goode T, Bell P, Richman LK, and Wilson JM. Severe toxicity in nonhuman primates and piglets following high-dose intravenous administration of an adeno-associated virus vector expressing human SMN. Hum Gene Ther. **29**: 285–298. 2018. [Medline] [CrossRef]
9. Hordeaux J, Wang Q, Katz N, Buza EL, Bell P, and Wilson JM. The neurotropic properties of AAV-PHP.B are limited to C57BL/6J mice. Mol Ther. **26**: 664–668. 2018. [Medline] [CrossRef]
10. Manini A, Abati E, Nuredini A, Corti S, and Comi GP. Adeno-associated virus (AAV)-mediated gene therapy for Duchenne muscular dystrophy: the issue of transgene persistence. Front Neurol. **12**: 814174. 2022. [Medline] [CrossRef]
11. Mueller C, Berry JD, McKenna-Yasek DM, Gernoux G, Owegi MA, Pothier LM, Douthwright CL, Gelevski D, Luppino SD, Blackwood M, Wightman NS, Oakley DH, Frosch MP, Flotte TR, Cudkowicz ME, and Brown RH Jr. SOD1 suppression with adeno-associated virus and microRNA in familial ALS. N Engl J Med. **383**: 151–158. 2020. [Medline] [CrossRef]
12. Furukawa S, Nagaike M, and Ozaki K. Databases for technical aspects of immunohistochemistry. J Toxicol Pathol. **30**: 79–107. 2017. [Medline] [CrossRef]
13. Moroki T, Matsuo S, Hatakeyama H, Hayashi S, Matsumoto I, Suzuki S, Kotera T, Kumagai K, and Ozaki K. Databases for technical aspects of immunohistochemistry:

2021 update. J Toxicol Pathol. **34**: 161–180. 2021. [Medline] [CrossRef]
14. Bhat N, and Fitzgerald KA. Recognition of cytosolic DNA by cGAS and other STING-dependent sensors. Eur J Immunol. **44**: 634–640. 2014. [Medline] [CrossRef]
15. Methatham T, Nagai R, and Aizawa K. A new hypothetical concept in metabolic understanding of cardiac fibrosis: glycolysis combined with TGF-β and KLF5 signaling. Int J Mol Sci. **23**: 4302. 2022. [Medline] [CrossRef]
16. Singh VP, Baker KM, and Kumar R. Activation of the intracellular renin-angiotensin system in cardiac fibroblasts by high glucose: role in extracellular matrix production. Am J Physiol Heart Circ Physiol. **294**: H1675–H1684. 2008. [Medline] [CrossRef]
17. Kim JJ, Lipatova Z, and Segev N. TRAPP complexes in secretion and autophagy. Front Cell Dev Biol. **4**: 20. 2016. [Medline] [CrossRef]
18. Civitarese RA, Talior-Volodarsky I, Desjardins JF, Kabir G, Switzer J, Mitchell M, Kapus A, McCulloch CA, Gullberg D, and Connelly KA. The α11 integrin mediates fibroblast-extracellular matrix-cardiomyocyte interactions in health and disease. Am J Physiol Heart Circ Physiol. **311**: H96–H106. 2016. [Medline] [CrossRef]
19. Yoshida H. [Golgi stress response]. Seikagaku. **89**: 154–163. 2017 (in Japanese). [Medline]
20. Baldrick P, McIntosh B, and Prasad M. Adeno-associated virus (AAV)-based gene therapy products: what are toxicity studies in non-human primates showing us? Regul Toxicol Pharmacol. **138**: 105332. 2023. [Medline] [CrossRef]
21. Yamashita T, Yamamoto T, Uchida E, and Inoue T. Immune responses involved in the efficacy and safety of gene therapy using adeno-associated virus vectors. Pharm Tech Jpn. **37**: 2645–2651. 2021.
22. Kuranda K, Jean-Alphonse P, Leborgne C, Hardet R, Collaud F, Marmier S, Costa Verdera H, Ronzitti G, Veron P, and Mingozzi F. Exposure to wild-type AAV drives distinct capsid immunity profiles in humans. J Clin Invest. **128**: 5267–5279. 2018. [Medline] [CrossRef]
23. Nidetz NF, McGee MC, Tse LV, Li C, Cong L, Li Y, and Huang W. Adeno-associated viral vector-mediated immune responses: Understanding barriers to gene delivery. Pharmacol Ther. **207**: 107453. 2020. [Medline] [CrossRef]
24. Shao W, Earley LF, Chai Z, Chen X, Sun J, He T, Deng M, Hirsch ML, Ting J, Samulski RJ, and Li C. Double-stranded RNA innate immune response activation from long-term adeno-associated virus vector transduction. JCI Insight. **3**: e120474. 2018. [Medline] [CrossRef]
25. Minamino T, Komuro I, and Kitakaze M. Endoplasmic reticulum stress as a therapeutic target in cardiovascular disease. Circ Res. **107**: 1071–1082. 2010. [Medline] [CrossRef]
26. Okada K, Minamino T, Tsukamoto Y, Liao Y, Tsukamoto O, Takashima S, Hirata A, Fujita M, Nagamachi Y, Nakatani T, Yutani C, Ozawa K, Ogawa S, Tomoike H, Hori M, and Kitakaze M. Prolonged endoplasmic reticulum stress in hypertrophic and failing heart after aortic constriction: possible contribution of endoplasmic reticulum stress to cardiac myocyte apoptosis. Circulation. **110**: 705–712. 2004. [Medline] [CrossRef]
27. Tsutsui H, Kinugawa S, and Matsushima S. Oxidative stress and heart failure. Am J Physiol Heart Circ Physiol. **301**: H2181–H2190. 2011. [Medline] [CrossRef]
28. Fong S, Handyside B, Sihn CR, Liu S, Zhang L, Xie L, Murphy R, Galicia N, Yates B, Minto WC, Vitelli C, Harmon D, Ru Y, Yu GK, Escher C, Vowinckel J, Woloszynek J, Akeefe H, Mahimkar R, Bullens S, and Bunting S. Induction of ER stress by an AAV5 BDD FVIII construct is dependent on the strength of the hepatic-specific promoter. Mol Ther Methods Clin Dev. **18**: 620–630. 2020. [Medline] [CrossRef]
29. Oslowski CM, and Urano F. Measuring ER stress and the unfolded protein response using mammalian tissue culture system. Methods Enzymol. **490**: 71–92. 2011. [Medline] [CrossRef]
30. Li X, Elwell MR, Ryan AM, and Ochoa R. Morphogenesis of postmortem hepatocyte vacuolation and liver weight increases in Sprague-Dawley rats. Toxicol Pathol. **31**: 682–688. 2003. [Medline] [CrossRef]
31. Reiling JH, Olive AJ, Sanyal S, Carette JE, Brummelkamp TR, Ploegh HL, Starnbach MN, and Sabatini DMA. A CREB3-ARF4 signalling pathway mediates the response to Golgi stress and susceptibility to pathogens. Nat Cell Biol. **15**: 1473–1485. 2013. [Medline] [CrossRef]
32. Taniguchi M, Nadanaka S, Tanakura S, Sawaguchi S, Midori S, Kawai Y, Yamaguchi S, Shimada Y, Nakamura Y, Matsumura Y, Fujita N, Araki N, Yamamoto M, Oku M, Wakabayashi S, Kitagawa H, and Yoshida H. TFE3 is a bHLH-ZIP-type transcription factor that regulates the mammalian Golgi stress response. Cell Struct Funct. **40**: 13–30. 2015. [Medline] [CrossRef]
33. Miyata S, Mizuno T, Koyama Y, Katayama T, and Tohyama M. The endoplasmic reticulum-resident chaperone heat shock protein 47 protects the Golgi apparatus from the effects of O-glycosylation inhibition. PLoS One. **8**: e69732. 2013. [Medline] [CrossRef]
34. Golebiowski D, van der Bom IMJ, Kwon CS, Miller AD, Petrosky K, Bradbury AM, Maitland S, Kühn AL, Bishop N, Curran E, Silva N, GuhaSarkar D, Westmoreland SV, Martin DR, Gounis MJ, Asaad WF, and Sena-Esteves M. Direct intracranial injection of AAVrh8 encoding monkey β-N-acetylhexosaminidase causes neurotoxicity in the primate brain. Hum Gene Ther. **28**: 510–522. 2017. [Medline] [CrossRef]